Fusion Engineering and Design 216 (2025) 115090

Contents lists available at ScienceDirect

Fusion Engineering and Design

journal homepage: www.elsevier.com/locate/fusengdes

Thermo-mechanical analysis of DTT Vacuum Vessel Thermal Shield

S. Del Nero [a], M. Fulici [a], G. Barone [b], R. Bonifetto [c,*], M. Dalla Palma [d,e], P. Fanelli [a]

[a] Department of Economy, Engineering, Society and Business Organization (DEIM), University of Tuscia, Largo dell'Università, Viterbo, 01100, Italy
[b] Department of Fusion and Technology for Nuclear Safety and Security – ENEA, Via Enrico Fermi 45, Frascati, 00044, Italy
[c] NEMO Group, Energy Department, Politecnico di Torino, Corso Duca degli Abruzzi 24, Torino, 10129, Italy
[d] Istituto per la Scienza e Tecnologia dei Plasmi, CNR, Corso Stati Uniti 4, Padova, 35127, Italy
[e] Consorzio RFX (CNR, ENEA, INFN, Università di Padova, Acciaierie Venete SpA), Corso Stati Uniti 4, Padova, 35127, Italy

ARTICLE INFO

Keywords:
DTT
Vacuum Vessel
Thermal Shield
Thermo mechanical analysis

ABSTRACT

The Thermo-structural behavior of the Vacuum Vessel (VV) and Vacuum Vessel Thermal Shield (VVTHS) of the Divertor Tokamak Test (DTT) project under thermal loads and piping-induced stresses was evaluated using Finite Element Analysis (FEA). The THS consists of two shells, respectively referred as inner THS and outer THS, with Cooling Pipes (CPs) welded to the innermost. The VV and THS are mechanically coupled by using bolts that constrain relative displacements. A Finite Element Model (FEM) was developed using shell elements for VV and VVTHS, beam elements for CPs and bolts, and coupling equations to simulate bolted connections. The analysis incorporated temperature-dependent material properties and periodic cycling conditions for applied on VV. Results provide insight into the displacement and stress distributions across the components, informing the structural integrity and future design optimization of the DTT VVTHS system.

1. Introduction

The Divertor Tokamak Test (DTT) facility is an Italian project designed to address one of the most critical challenges in magnetic confinement fusion: the effective management of heat and particle fluxes. As part of a larger effort to develop viable fusion reactors, the DTT focuses on testing advanced divertor configurations and related technologies under conditions that mimic those of a full-scale reactor. The facility plays a pivotal role in understanding plasma-material interactions and in evaluating potential designs for future power plants [1].

A crucial component of the DTT system is the THS, which is designed to minimize heat transfer between the VV and the superconducting magnets system that will operate at 4.5 K [2]. In fact, the VVTHS ensures thermal insulation by reflecting radiative heat and reducing conductive pathways, thus protecting temperature sensitive components [3]. The design and performance of THS have been extensively studied in major fusion projects, such as ITER and JT-60SA. The ITER THS, for example, is actively cooled with helium gas and incorporates low-emissivity coatings to reduce radiative heat transfer by over two orders of magnitude, protecting superconducting magnets operating at cryogenic temperatures [4]. Similarly, the JT-60SA THS employs a double-walled structure with helium cooling lines and relies on precise manufacturing and assembly tolerances to accommodate thermal and seismic loads [5]. Previous works have also highlighted the importance of detailed thermal-structural analyses in optimizing THS designs. For instance, transient and steady-state thermal analyses of the ITER shield validated its radiation shielding performance and informed simplifications for computational models [6]. These studies emphasize that achieving the required thermal performance often demands innovative engineering solutions, such as insulated couplers and modular design approaches.

The work presented in this study is integral to the Vacuum Vessel THS design process, providing critical insights into its thermo-structural behavior under operational conditions. By evaluating the displacement and stress fields resulting from thermal loads, this study aims to verify structural integrity and inform potential design optimizations. FEA is employed using ANSYS FE software to simulate realistic operating scenarios, incorporating temperature-dependent material properties for enhanced accuracy and reliability in performance predictions. The findings of this study contribute to ensuring the reliability and efficiency of the DTT THS, which supports the broader goals of the facility in advancing fusion technology.

2. Layout of DTT vacuum vessel thermal shield

The THS system is divided into three sub-assemblies: the Vacuum Vessel Thermal Shield, the Port Thermal Shield, and the Cryostat

* Corresponding author.
E-mail address: roberto.bonifetto@polito.it (R. Bonifetto).

https://doi.org/10.1016/j.fusengdes.2025.115090
Received 17 January 2025; Received in revised form 20 March 2025; Accepted 11 April 2025
Available online 27 April 2025
0920-3796/© 2025 The Authors. Published by Elsevier B.V. This is an open access article under the CC BY-NC-ND license (http://creativecommons.org/licenses/by-nc-nd/4.0/).

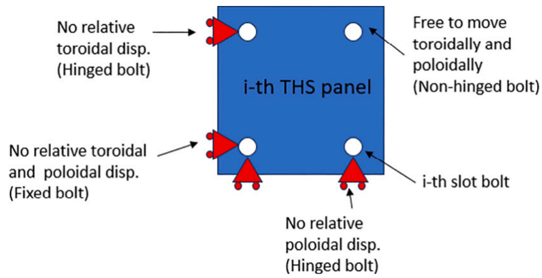

Fig. 1. Mechanical scheme of bolt connections.

Thermal Shield. The VVTHS is further segmented into 18 electrically insulated toroidal sectors, each spanning 20°, with multiple cooling modules.

Structurally, each 20° sector of the DTT Vacuum Vessel VVTHS, in turn divided into five non-continuous panels in the poloidal direction (two at the inboard, three at the outboard), is composed of two shells. These are referred to as the inner THS and outer THS, and they are connected to the VV through a bolt system that constrains relative displacements while allowing controlled thermal expansion.

The CPs, integrated with the inner VVTHS, are welded along its surface and feature bellows at the gaps between adjacent panels, ensuring free thermal contraction of the THS system. The cooling circuit consists of 15 independent helium lines: 6 lines cool the inboard panels (each line cools three sectors in series), and 9 lines cool the outboard ones (each cools two sectors in series); the 15 lines are running in parallel to maintain uniform cooling performance, and each of them is then doubled for redundancy [2].

For simplicity, the Vacuum Vessel THS will be referred to as the THS in this work.

3. FE model

The thermo-mechanical behavior of the THS is analyzed through FE simulations conducted using the ANSYS software. Due to thin thicknesses, both VV and THS were modeled using linear shell elements (SHELL181), while linear beam elements for both bolts and CPs were considered (BEAM188) [7,8]. The VV and THS are coupled by the presence of several bolts referred as fixed, hinged and non-hinged. Fixed bolts do not allow relative displacement and directly anchor the THS onto VV, meanwhile hinged bolts allow either relative poloidal or toroidal displacement, and non-hinged bolts permit both poloidal and toroidal relative displacement. All bolts are fixed to the VV and prevent local relative displacement of the THS shells along their own axis while allowing free rotation around the same axis. A simplified and schematic overview of how bolts are coupled to one of the outer THS panels is shown in Fig. 1, while the bolt arrangement on both VV and THS is shown in Fig. 2.

For each panel of the outer THS, one fixed bolt is required to properly constrain it. After choosing which of the set of bolts in the individual panel will be the fixed one, the remaining hinged to non-hinged bolts can be determined. Bolts in the same poloidal plane as the fixed one will allow only relative displacements in the poloidal direction, while those having the same poloidal angle as the fixed one will allow only relative toroidal displacements, and the remainder will allow both relative displacements (see Fig. 3). Differently from the outer THS for which one fixed bolt per panel is required, the two CPs welded on the inner THS connect the panels on the inner and outer sides respectively, forming two unified structures. Consequently, one fixed bolt is used for inboard and one for the outboard side. Following a similar approach used for bolts on the outer THS, the distinction between hinged and non-hinged bolts can also be established for the inner THS (see Fig. 4).

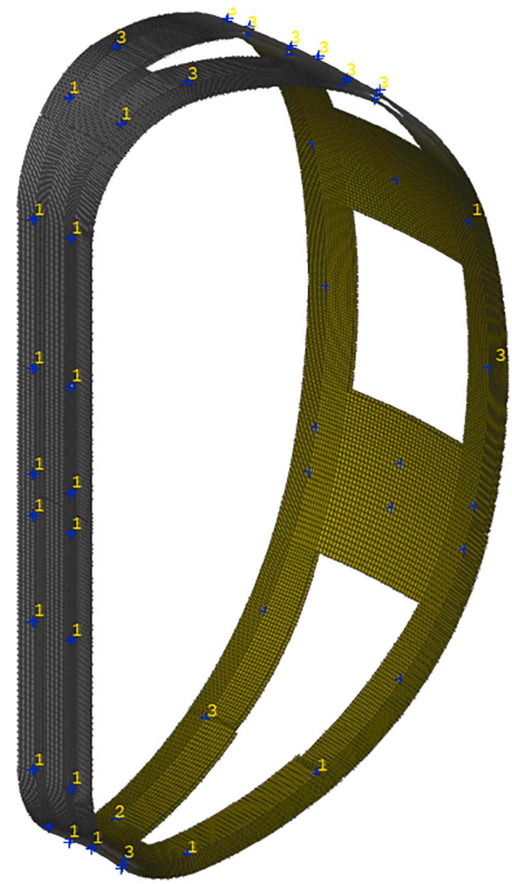

Fig. 2. Bolts arrangement (highlighted in blue) on VV and THS.

Table 1
SS 316LN mechanical properties.

T [°C]	E [GPa]	ν	α [μm/(m °C)]	λ [W/(m °C)]
−193	210	0.3	13.3	9.2
+60	193	0.3	16.3	15.0
+200	183	0.3	16.8	17.0

As previously mentioned, two CPs flow along the inboard and outboard sides of the inner THS, effectively cooling it and preventing excessive heat flux from reaching the superconducting magnet system. To allow thermal contractions without inducing peak stresses and flexural effects on THS, between each panel bellows have been introduced. The extension of the bellows is along the toroidal direction, and their length was changed to understand their influence on the behavior of the whole assembly during the application of thermal loads. The two CPs and bellows are shown in Fig. 5 and in Fig. 6.

The VV is subject to periodic cycling condition, while the mechanical properties of the material change with the temperature. Here, no transient effects related to reaching the target temperatures for VV and THS were considered; in this context, the assumption was made of the achievement of thermal equilibrium and uniform and homogeneous temperatures on the various components. Although this introduces an approximation, it is a reasonable simplification at this conceptual design stage, where the focus is on evaluating the overall structural behavior under thermal load conditions.

The thicknesses of the VV, inner THS, and outer THS are 15 mm, 2 mm, and 1 mm, respectively. The internal and external diameters of CPs are 9.24 mm and 13.72 mm respectively, while the bolt diameter is 12 mm. The initial gap without applied loads between VV and inner THS is 20 mm, meanwhile it is 13.72 mm (the same as the external

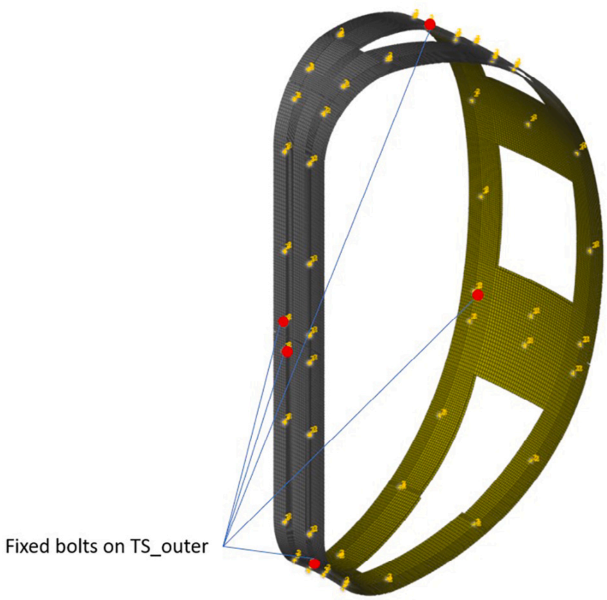

Fig. 3. Positions of the fixed bolts on the outer THS.

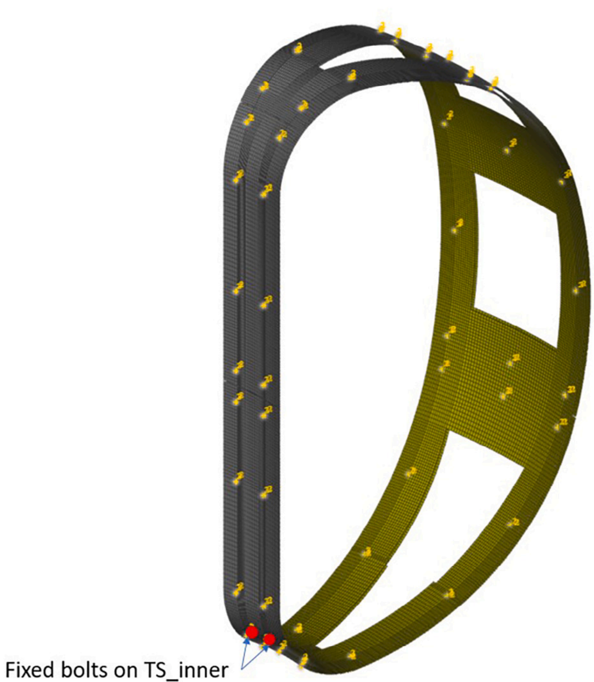

Fig. 4. Positions of the fixed bolts on the inner THS.

Table 2
G10-CR mechanical properties.

T [°C]	E [GPa]	ν	α [μm/(m °C)]	λ [W/(m °C)]
−269	35.9	0.210	20.62	0.025
−196	33.7	0.183	20.64	0.100
+22	28.0	0.144	3.06	0.500

diameter of CPs) between the inner and outer THS. The gaps are maintained by the presence of the bolts, which also serve to ensure proper spacing between the various components by preventing them from coming into contact.

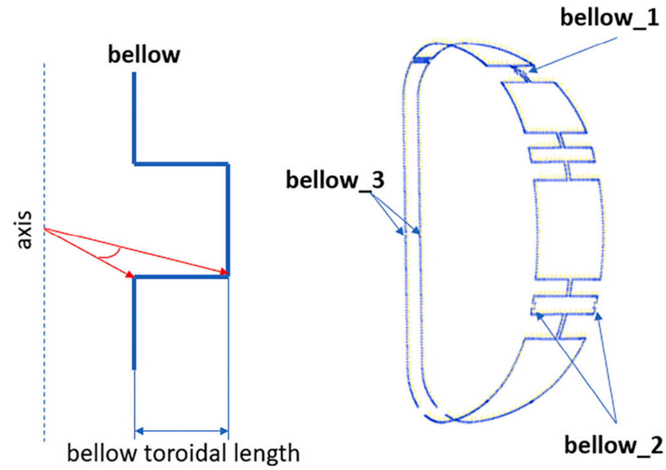

Fig. 5. Representation of Cooling Pipes (CPs) and bellows.

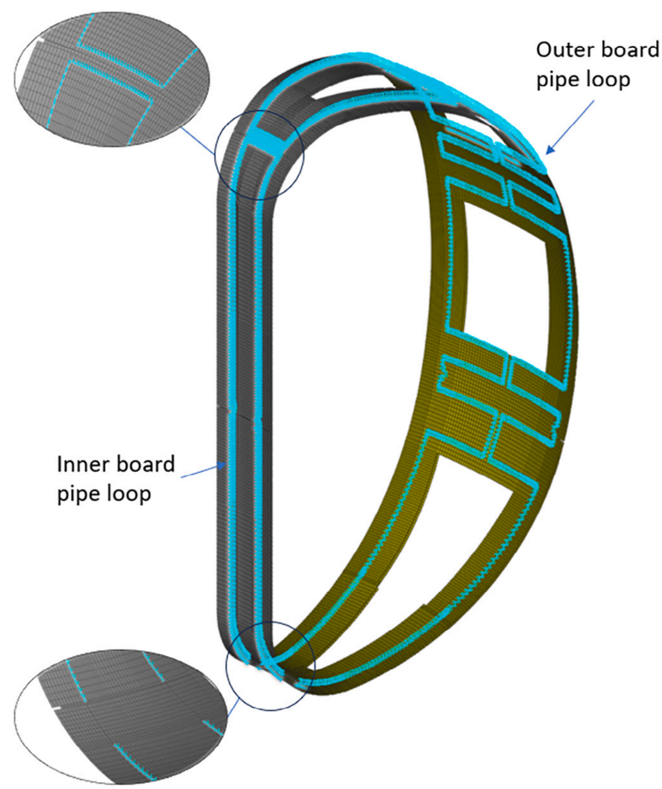

Fig. 6. Representation of cooling pipes, bellows, VV and inner THS.

The VV, THS, and CPs are constructed from SS 316LN, with their corresponding mechanical properties detailed in Table 1 [9–12]. Conversely, the bolts are made of G10-CR, a material chosen for its ability to prevent electrical currents from flowing between the VV and the remaining components [13,14]. Table 2 presents the mechanical properties of G10-CR used in the FEA, shown as a function of temperature. Due to the limited availability of mechanical properties data for the materials at certain evaluation points, interpolation was employed to estimate the missing values, ensuring an accurate representation of the properties at the operating temperatures of the various components. Furthermore, the beam element formulation used to model the bolts results in a simplified stress–strain tensor, and some orthotropic material properties are actually neglected. Therefore, Young's modulus $E_{lengthwise}$, Poisson's ratio $\nu_{crosswise}$, coefficient of thermal expansion $\alpha_{lengthwise}$ and thermal conductivity coefficient $\lambda_{lengthwise}$ were considered for G10-CR.

4. Load conditions

The evaluated cases are summarized in Table 3. Temperature conditions are assumed constant and uniformly distributed over the various components.

Table 3
Thermal load conditions.

Case	T_{VV} [°C]	$T_{THSinner}$ [°C]	$T_{THSouter}$ [°C]	l [mm]
1a	60	−166	−193	50
1b	60	−166	−193	75
1c	60	−166	−193	90
2a	200	−159	−181	50
2b	200	−159	−181	75
2c	200	−159	−181	90

Where l represents the length of all bellows in toroidal direction, T_{VV}, $T_{THSinner}$ and $T_{THSouter}$, respectively, the temperature applied on VV, inner THS and outer THS. Being CPs welded on the inner THS, the same temperature have been used, while the bolts are subjected to a thermal gradient due to different temperatures on the inner THS, outer THS and VV. Thus, as can be seen from Table 3, two main scenarios (1^{st} and 2^{nd}) were analyzed, and displacement and stress fields were evaluated for each of them as the bellows extension changed. The temperatures applied to the structural components in this study are derived from preliminary analyses conducted as part of the DTT design process. These temperatures are informed by a combination of heat transfer simulations, engineering approximations, and iterative design feedback. Although the specific numerical values may differ slightly from those presented in earlier works, such as those highlighted in [15], the general trends and boundary conditions remain consistent.

5. Thermo-mechanical analysis

The objective of these analyses is to assess the deformation of the VV and THS under thermal loads, considering the presence of the CPs while varying the bellow lengths and evaluating the relative distances (gaps) between VV, inner THS and outer THS. The analyses reveal that the toroidal length of the bellows has minimal impact on the displacement and stress distributions of the VV, inner THS, outer THS, CPs and bolts. For the same temperature conditions, these distributions remain virtually unchanged. This stability is attributed to the structural connections, which were appropriately chosen to minimize the thermal contraction effects of the CPs. The inner THS is secured to the VV via two fixed bolts (forming two joined structures, one at the inboard and one at the outboard, due to the CPs), while the outer THS is attached to the VV by five fixed bolts, one per panel. The displacement and stress field are then provided for each of the two scenarios analyzed.

The VV exhibits a maximum displacement ranging from 2 mm to 11 mm across the scenarios (see Figs. 7 and 13) with induced stresses varying between 1 MPa and 2 MPa (see Figs. 10 and 16). These stress levels are negligible and well within acceptable limits, indicating the structural integrity of the VV under the imposed conditions.

The inner THS shows its maximum displacement and stress at the top outboard region. The displacement increases from 22 mm to 42 mm (see Figs. 8 and 14), while the corresponding stress rises from 13 MPa to 22 MPa (see Figs. 11 and 17). Conversely, the outer THS experiences maximum displacement at the central outboard panel, ranging from 11 mm to 21 mm (see Figs. 9 and 15). The peak stress for the outer THS, however, is observed at the bottom inboard panel, where it increases slightly from 7 MPa to 10 MPa (see Figs. 12 and 18). The stress distribution in the outer THS is primarily influenced by the curvature changes induced by thermal contraction and the constraint imposed by the bolts, which restrict axial movement.

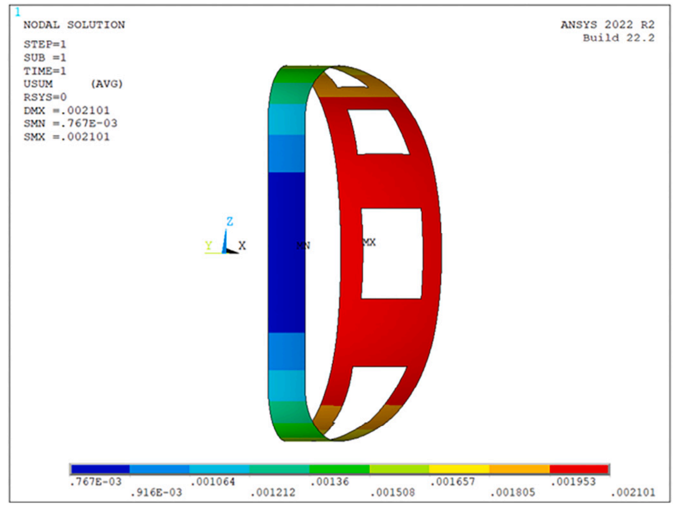

Fig. 7. VV displacement field of 1st thermal load case [m].

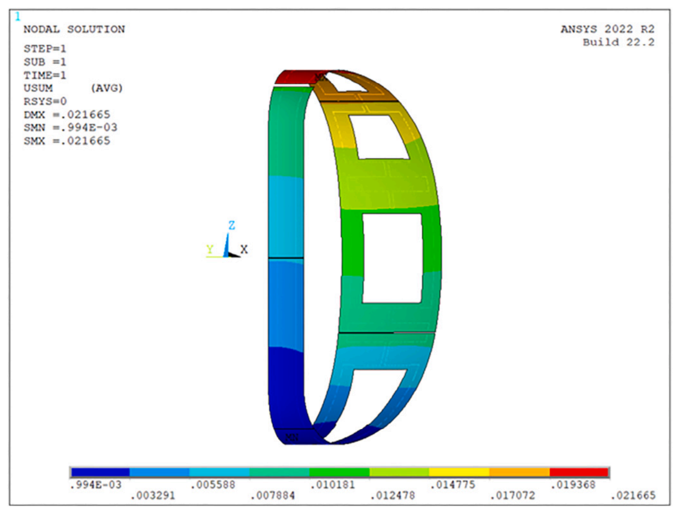

Fig. 8. Inner THS displacement field of 1st thermal load case [m].

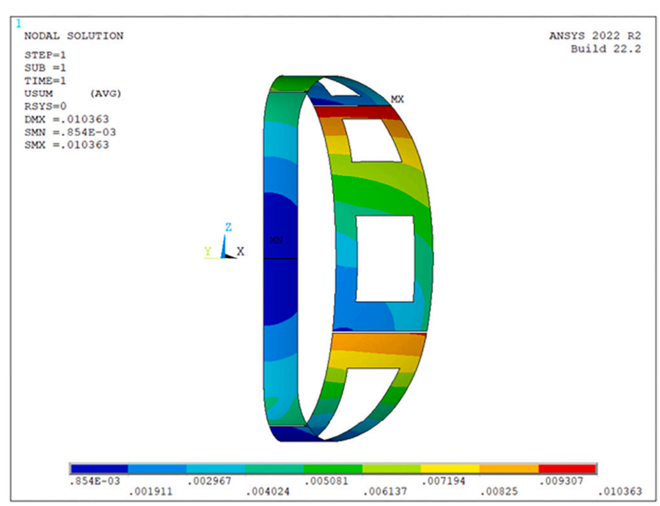

Fig. 9. Outer THS displacement field of 1st thermal load case [m].

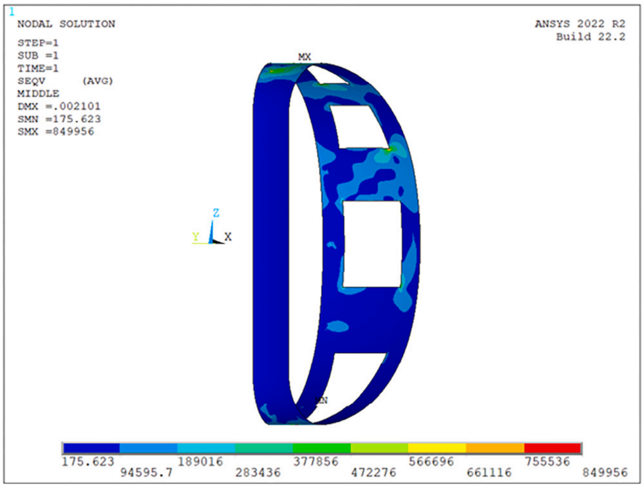

Fig. 10. VV stress field of 1st thermal load case [Pa].

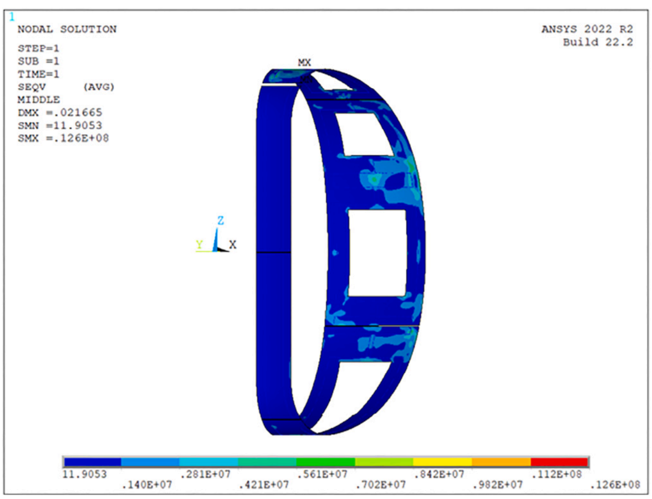

Fig. 11. Inner THS stress field of 1st thermal load case [Pa].

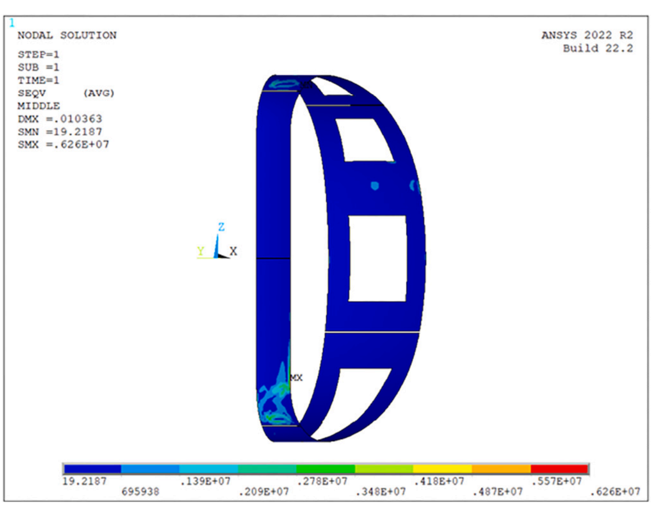

Fig. 12. Outer THS stress field of 1st thermal load case [Pa].

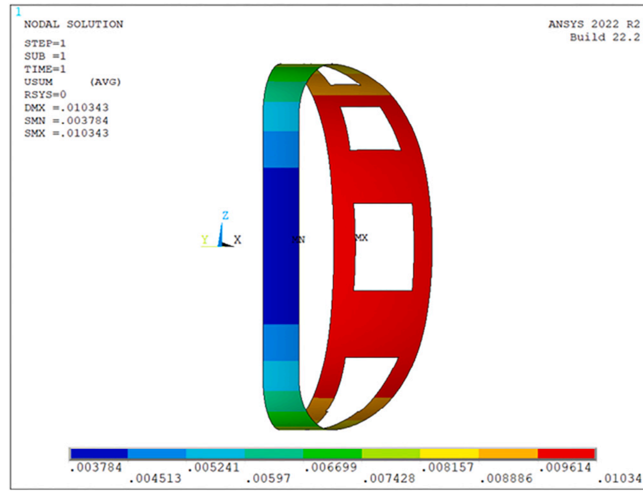

Fig. 13. VV displacement field of 2nd thermal load case [m].

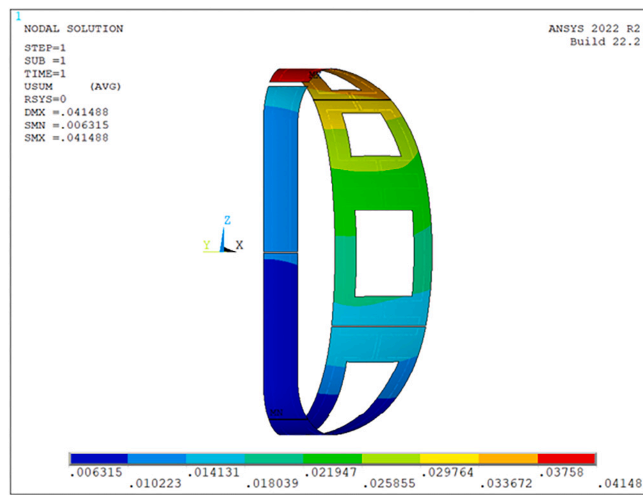

Fig. 14. Inner THS displacement field of 2nd thermal load case [m].

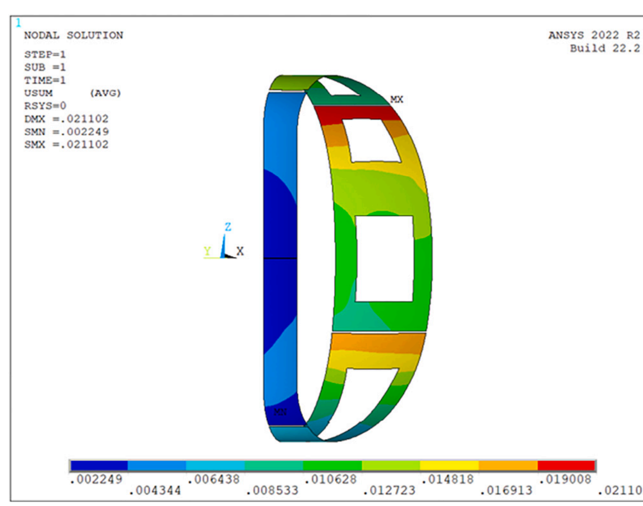

Fig. 15. Outer THS displacement field of 2nd thermal load case [m].

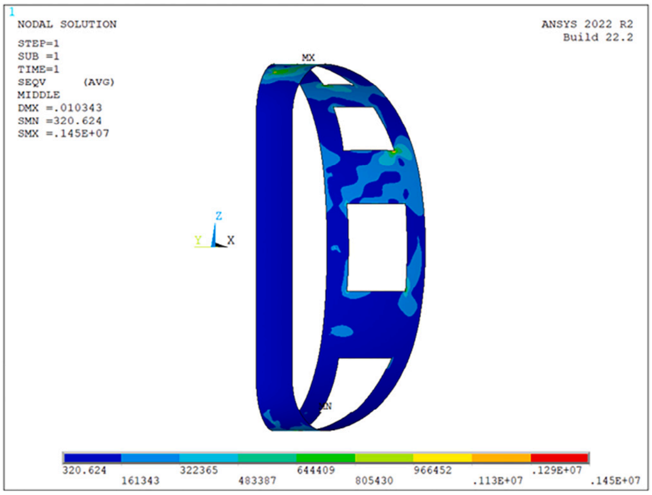

Fig. 16. VV stress field of 2nd thermal load case [Pa].

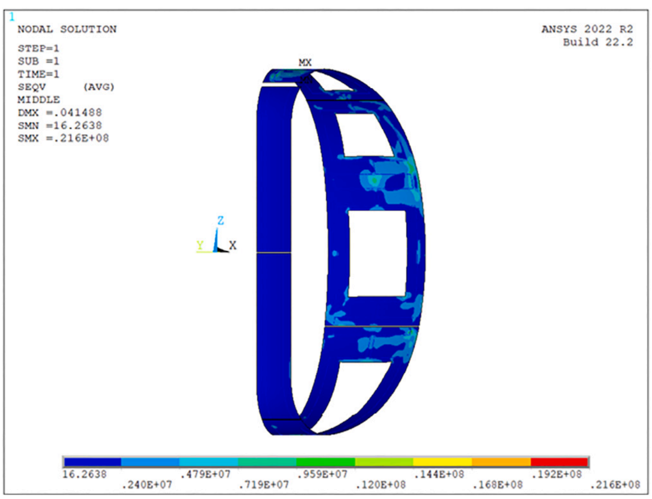

Fig. 17. Inner THS stress field of 2nd thermal load case [Pa].

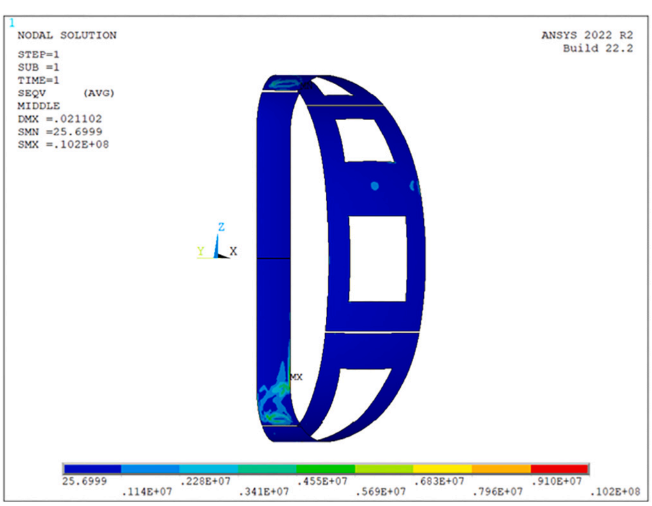

Fig. 18. Outer THS stress field of 2nd thermal load case [Pa].

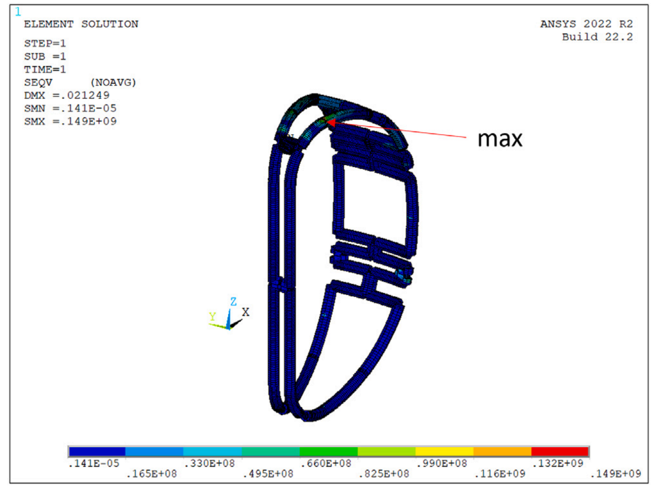

Fig. 19. Stress distribution in CPs for 1st thermal load case [Pa].

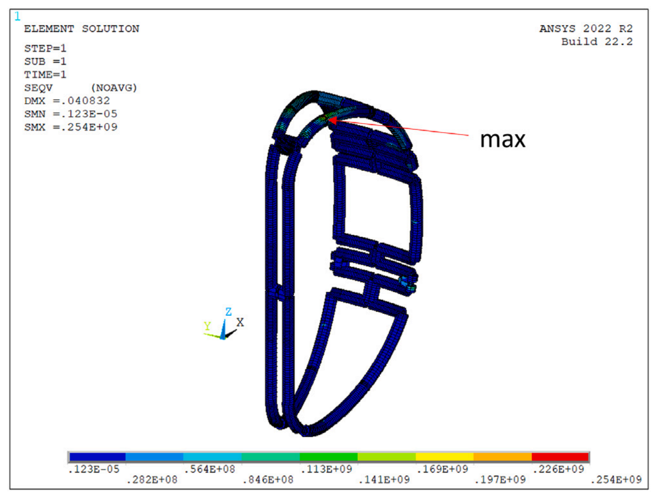

Fig. 20. Stress distribution in CPs for 2nd thermal load case [Pa].

For the CPs, the displacement field closely follows that of the inner THS, except for the bellows, which are free to move and thus exhibit slightly distinct behavior. The peak stress in the CPs reaches 150 MPa in the first scenario (see Fig. 19) but nearly doubles in the second scenario, reaching approximately 260 MPa (see Fig. 20).

The bolts exhibit peak stress at the top outboard connection for each analyzed scenario. The stress in these bolts increases significantly, from 108 MPa in the first scenario to 183 MPa in the second scenario, reflecting the amplified structural demands under the higher thermal loads.

Overall, the results indicate that while the VV and THS components exhibit only minor stress increase, the CPs and bolts are subjected to considerable stress variations. These findings highlight the need for careful design considerations for these elements, particularly under increased thermal loads, to ensure the structural integrity and longevity of the DTT system.

Another key outcome of the analysis is the evaluation of the relative distances between the VV, inner THS, and outer THS, which are critical for ensuring that no local contact areas form due to thermal deformations. Such contact could compromise the operability and functionality of the system.

As shown in Figs. 21 and 22, the distributions of relative distances remain largely unaffected by variations in thermal loads and bellows extension.

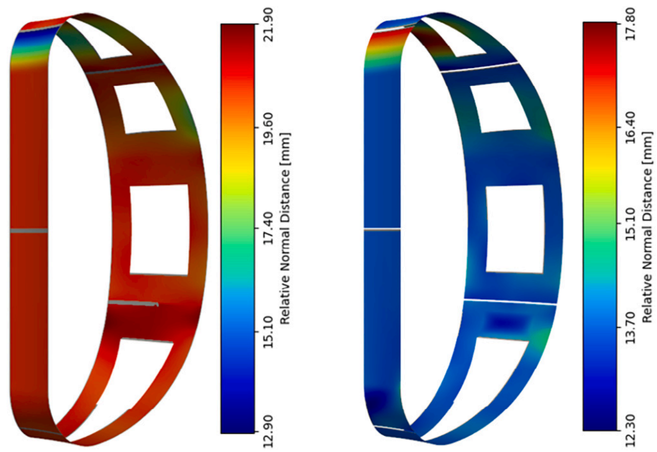

Fig. 21. Stress distribution in CPs for 1st thermal load case [Pa].

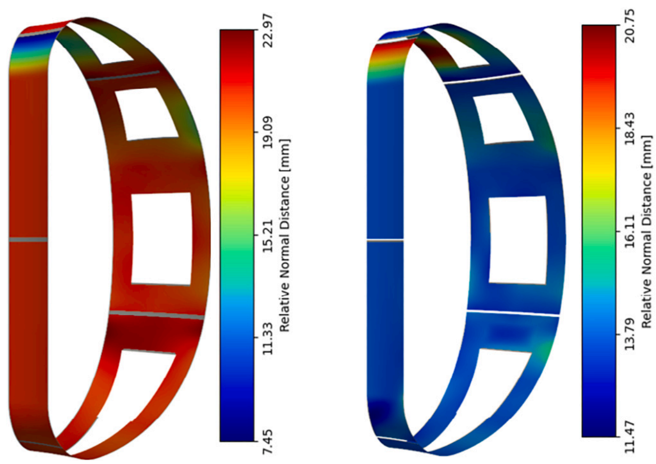

Fig. 22. Stress distribution in CPs for 2nd thermal load case [Pa].

The minimum distance between the VV and the inner THS is observed at the top inboard region, decreasing from approximately 13 mm to 8 mm across the evaluated scenarios. For most areas, however, the gap remains close to the initial value of 20 mm, with slight reductions to around 18 mm at the top outboard and in the center panel of the outboard.

The gap between the inner THS and the outer THS remains virtually unchanged from its initial value of 13.72 mm. Nevertheless, a slight receding of the outer THS is noted at the inboard and outboard tops, where the gap increases to approximately 18 mm, and a slight approach to the bottom inboard where the gap drops to about 11 mm. The reduction of the gap between inner and outer THS in some places is due of the simplified modeling used, in fact the CPs are in contact only with the inner THS and not with the outer THS. In reality the CPs are in contact with both shells, and this will lead to a larger gap than calculated.

6. Conclusions

This study investigated the thermo-mechanical behavior of the Vacuum Vessel (VV) and Thermal Shield (THS) components in the Divertor Tokamak Test (DTT) system under different thermal loading scenarios. Key objectives included evaluating displacement and stress distributions in the VV, inner THS, outer THS, Cooling Pipes (CPs), and bolts, as well as examining the relative distances (gaps) between the three shells.

The findings revealed that the toroidal length of the bellows had a negligible impact on the displacement and stress distributions of the VV, THS, and other structural components. This behavior is attributed to the robust bolted connections in order to reduce the impact of CPs during their thermal contraction. Two fixed bolts anchor the inner THS to the VV, creating two joined structures at the inboard and outboard regions due to the CPs, while five fixed bolts secure the outer THS to the VV, one for each panel.

Although displacement and stress distributions remained consistent across all scenarios, the analyses identified the bolts and CPs as critical components due to their significant stress levels, reaching 183 MPa and 260 MPa, respectively. Furthermore, the maximum stress on the CPs and bolts is acceptable, but it is undoubtedly necessary to employ more detailed models to capture the real stress condition acting on these components. In fact, modeling the CPs and bolts through beam elements is a simplification useful only in understanding the behavior of the entire structure and how the various components interact with each other.

Relative gaps between the VV, inner THS, and outer THS were largely maintained, with only minor variations. The analysis confirmed that no contact occurs between the shells under the imposed thermal loads, preserving the system's operability.

Future research should focus on optimizing the number, location, and dimensions of the bolts to allow for controlled contraction and expansion of the components, thereby reducing localized stress concentrations. Additionally, the assumption of uniform component temperatures should be refined by including thermal gradients resulting from heat transfer through the cooling pipes. This enhanced modeling approach could provide a deeper understanding of the thermo-mechanical behavior and support the further optimization of the DTT system.

Abbreviations

- DTT: Divertor Tokamak Test
- VV: Vacuum Vessel
- THS: Thermal Shield
- FEA: Finite Element Analysis
- CPs: Cooling Pipes
- FEM: Finite Element Model
- ITER: International Thermonuclear Experimental Reactor
- JT-60SA: Japan Torus-60 Super Advanced
- SS 316LN: Stainless Steel 316LN
- G10-CR: Fiberglass composite material
- T_{VV}: Temperature of Vacuum Vessel
- $T_{THSinner}$: Temperature of inner Thermal Shield
- $T_{THSouter}$: Temperature of outer Thermal Shield
- l: length of the bellows in toroidal direction

CRediT authorship contribution statement

S. Del Nero: Writing – original draft, Software. **M. Fulici:** Software. **G. Barone:** Project administration, Conceptualization. **R. Bonifetto:** Project administration, Conceptualization. **M. Dalla Palma:** Project administration, Conceptualization. **P. Fanelli:** Supervision, Methodology.

Declaration of competing interest

The authors declare that they have no known competing financial interests or personal relationships that could have appeared to influence the work reported in this paper.

Acknowledgments

This work is carried out in the frame of the DTT activity. The authors are very grateful to all the colleagues involved in the DTT project for their precious contributions.

Data availability

The data that has been used is confidential.

References

[1] R. Martone, et al., DTT Divertor Tokamak Test Facility Interim Design Report, ENEA, 2019.

[2] G. Barone, S. Roccella, E. Martelli, E. Visca, DTT thermal shield: Preliminary thermal analysis, Fusion Eng. Des. (2020).

[3] B. Končar, O. Costa Garrido, M. Draksler, R. Brown, C. Bachmann, Development of DEMO thermal shield concept: Design requirements and expected thermal loads, in: 26th International Conference Nuclear Energy for New Europe.

[4] V. Bykov, The thermal shields for the ITER magnet system: thermal, structural and assembly aspects, Fusion Eng. Des. (2001).

[5] S. Nakamura, Design and manufacturing of thermal shield for JT-60SA, Fusion Eng. Des. (2019).

[6] K. Nam, et al., Thermal analysis on detailed 3D models of ITER thermal shield, Fusion Eng. Des. (2014).

[7] ANSYS Element Reference, Release 2021 R2.

[8] ANSYS Theory Reference, Release 2021 R2.

[9] Ansys Granta Selector, Stainless steel, austenitic, AISI 316LN, annealed, 2022.

[10] L.F. Li, Y.T. Zhang, Y.Y. Li, Development of cryogenic structural materials, in: Proceedings of the Twentieth International Cryogenic Engineering Conference, ICEC 20, Beijing, China, 2005.

[11] J.H. Kim, J. Feng, The 4K mechanical properties of modified SS316LN for jacket materials in superconducting fusion magnets, AIP Conf. Proc. 986 (2008) 92–99.

[12] J. Sas, K.-P. Weiss, A. Jung, The mechanical and material properties of 316LN austenitic stainless steel for the fusion application in cryogenic temperatures, IOP Conf. Ser.: Mater. Sci. Eng. (2003).

[13] M.B. Kasen, G.R. MacDonald, D.H. Beekman Jr., R.E. Schramm, Mechanical, Elcrtical, and Thermal Characterization of G-10CR and G-11CR Glass-Cloth/Epoxy Laminates Between Room Temperature and 4K, National Bureau of Standards, Boulder, Colorado.

[14] Y. Shindo, K. Horiguchi, R. Wang, Cryomechanics and short-beam interlaminar shear strength of G-10CR glass-cloth/epoxy laminates, 2000.

[15] R. Bonifetto, G. Barone, V. Belardi, M. Della Palma, M. De Bastiani, S. Del Nero, P. Fanelli, M. Micheletti, G. Ventura, G. Zavarise, Design of the thermal shield for the DTT facility, in: 33rd Symposium on Fusion Technolgy, 2024.